Fragmentation of small tin cluster ions (Sn x + : x=4–20) in the low-energy collisions with a highly oriented pyrolytic graphite surface

Yutaka Tai, Junichi Murakami, Chiranjib Majumder, Vijay Kumar, Hiroshi Mizuseki, and Yoshiyuki Kawazoe

Citation: The Journal of Chemical Physics **117**, 4317 (2002); doi: 10.1063/1.1496470
View online: http://dx.doi.org/10.1063/1.1496470
View Table of Contents: http://scitation.aip.org/content/aip/journal/jcp/117/9?ver=pdfcov
Published by the AIP Publishing

Fragmentation of small tin cluster ions (Sn_x^+: $x=4-20$) in the low-energy collisions with a highly oriented pyrolytic graphite surface

Yutaka Tai[a] and Junichi Murakami
Chubu Research Base, National Institute of Advanced Industrial Science and Technology (AIST), Nagoya 463-8560, Japan

Chiranjib Majumder,[b] Vijay Kumar,[c] Hiroshi Mizuseki, and Yoshiyuki Kawazoe
Institute for Materials Research, Tohoku University, Sendai 980-8577, Japan

(Received 18 March 2002; accepted 4 June 2002)

Fragmentation of tin cluster ions (Sn_x^+: $x=4-20$) in the low-energy collisions with a HOPG surface has been investigated by means of a tandem time of flight mass spectrometer for the incident energy range of 0–300 eV. At low incident energies, smaller clusters ($x\leqslant 11$) fragmented by the atom loss process, whereas larger clusters ($x>11$) decayed by fission. The favored fragmentation paths were similar to those for Si and Ge cluster ions. The results support the structural similarities among Si, Ge, and Sn clusters in the present size range. The low-energy fragmentation patterns were compared with those obtained from theoretical calculations using generalized gradient approximation (GGA) and the B3PW91 exchange–correlation functional. It has been found that the B3PW91 hybrid functional results are consistent with the experimental observations. © *2002 American Institute of Physics.* [DOI: 10.1063/1.1496470]

I. INTRODUCTION

Although C, Si, Ge, Sn, and Pb constitute a single row, the group-14 in the periodic table, bonding characteristics differ considerably from element to element. This is indeed reflected in the bulk structures and properties of these elements. Carbon is characterized by the multiplicity of its chemical bondings and because of this, several different structures such as diamond, graphite, fullerenes, nanotubes, are found to exist. It is now well known that these allotropes show quite different physical and chemical properties.[1] Silicon and germanium take the diamond structure, and are typical semiconductors. In contrast, tin (β-Sn) and lead, having tetragonal and cubic structures, respectively, show metallic properties. Thus, there is a semiconductor to metal transition between germanium and tin. However, at low temperatures ($\leqslant$286 K), β-Sn transforms to α-Sn (tin pest), a semiconductor phase. From this point of view, α-Sn is more like silicon and germanium than lead. The similarities and differences in crystal structures and physical properties among bulk Si, Ge, Sn, and Pb are well known, however, for clusters of these elements, they are not well understood.

The structures and properties of the clusters of group-14 elements have been subjects of intensive research during the last decade because of their importance in fundamental as well as applied science. A lot of studies have been done to clarify similarities and differences among Si, Ge, Sn, and Pb clusters, including covalent to metallic transition, and as shown in the following examples, some of them have presented controversial results.

From photoionization mass spectroscopy, it was pointed out that, though these clusters have a common magic number, $x=10$, implying covalent interactions among the constituent atoms, the abundance patterns of Sn and Pb clusters, to some extent, exhibited characteristics of densely packed geometries[2] which are commonly observed for clusters of transition metal elements.[3] An *ab initio* calculation did not show much differences between the structures of the lowest energy states of Sn_x and Pb_x ($x=3-10$).[4] These results support the structural similarities between Sn and Pb clusters. However, in contrast to these, photoelectron spectroscopy (PES) revealed different electronic band structures of Sn and Pb cluster anions.[5,6] The PE spectra observed for Sn_x^- were similar to those of Si_x^- and Ge_x^-, which is consistent with a density functional calculation suggesting similar ground state structures for Si_x, Ge_x, and Sn_x.[7] On the other hand, the PE spectra of Pb_x^- was indicative of electronic shell closing, and the size dependence of the electron detachment threshold showed a trend predicted by the jellium model.

Concerning structures of the group-14 clusters, detailed information has recently become available from ion-mobility measurements. For carbon clusters, a variety of isomers have been found (linear chain, ring, polycyclic ring, fullerene, tadpole, etc.).[8,9] It was revealed that silicon and germanium clusters adopt prolate growth up to $x\approx 30$ and then start to have spherical geometries as they grow further.[10,11] Shvartsburg and Jarrold have reported the summary of their gas-phase ion mobility measurements on $Si_x^+-Pb_x^+$, and concluded that noncompact to compact structural transition occurs between tin and lead in the small cluster systems ($x\leqslant 25$).[11]

Theoretical calculations also support the prolate growth,

[a]Author to whom correspondence should be addressed; electronic mail: tai.y@aist.go.jp
[b]Permanent address: Bhabha Atomic Research Center Munbai 400085, India.
[c]Permanent address: Dr. Vijay Kumar Foundation, 45 Bazaar Street, K. K. Nagar (West), Chennai 400078, India.

in which the tricapped trigonal prism (TTP) structure is the building block, for Si_x, Ge_x, and Sn_x (x up to 20), though the structures of the clusters are not precisely the same.[12–14] However, since, in general, a predicted structure may not be the one in the global energy minimum, comparison of the derived properties with experimental results would be needed to check the reliability of calculation.

In this paper, we present results of surface-induced dissociation (SID) of Sn_x^+ (x up to 20) on a highly oriented pyrolytic graphite (HOPG) surface. It is often the case that metal and semiconductor clusters dissociate by unimolecular decay in low energy SID, and the dissociation patterns correlate with the thermal stability of the fragment ions and their neutral counterparts.[15–17] It is, therefore, expected that, by comparing the SID results for Sn cluster ions with the SID and CID (collision induced dissociation) profiles of Si_x^+ and Ge_x^+, similarities and differences among these clusters can be deduced from the point of view of the fragmentation energetics. We have already reported some of the Sn_x^+ SID results in the small size range, and pointed out the similarity in the fragmentation patterns among Si_x^+, Ge_x^+, and Sn_x^+.[18] This paper will present a systematic study of the fragmentation behavior for x up to 20, and in addition, a comparison between the low-energy dissociation patterns and those obtained from *ab initio* calculations using generalized gradient approximation (GGA) and B3PW91 exchange–correlation functionals. Concerning the comparison of the dissociation pathways derived from experiment and theory, Shvartsburg *et al.* have demonstrated that it successfully works as a test for the global optimization of calculated structures of Si_x^+ (x up to 26).[19] Similar test for tin cluster cations is considered to be more challenging, since the binding energy per atom, and thus, energy differences among isomers are smaller.

II. EXPERIMENTAL METHODS

The experiments were performed by means of a home-designed tandem time-of-flight (TOF) mass spectrometer. The details of the experimental setup have been reported elsewhere, and are described here briefly.[17,20] Sn clusters were produced by the laser vaporization method: third harmonics of the Nd:YAG laser (pulse width, $\approx$7 ns; energy, 30–50 mJ/pulse) was focused on a Sn rod, synchronized with a pulsed He flow (stagnation pressure, 10 atm).[21] Positive ions from the cluster source were extracted by the Wiley–Mclaren's accelerator.[22] Mass spectra were obtained with a linear TOF mode. For the SID experiments, mass selection was performed by applying a pulsed high voltage (pulse width ≈ 2 μs) to a 90° ion mirror.[23,24] The mass selected ions were decelerated and allowed to collide with an HOPG surface. Scattered positive ions were then extracted back by the electric field with which the incident ions were decelerated, and were detected by a tandem microchannel plate. The collision energy was varied by changing a bias voltage at the substrate. The incident energy spread of the primary ion beam was estimated to be 80 eV (FWHM). In this paper, an incident energy (E_i) stands for the difference between the mean kinetic energy of the projectile ions and the substrate potential.

The experiment was carried out under UHV conditions: the base pressure in the scattering chamber was on the order of 10^{-9} Torr. The substrate was cleaved in air by the Scotch tape method before it was set in the vacuum system. During the experiments, the substrate was maintained at 150 °C to avoid physisorption of residual gases in the vacuum chamber.[25,26]

III. COMPUTATIONAL METHODS

The ground state geometries of the neutral and charged clusters have been obtained using the ultrasoft pseudopotential method[27,28] with a plane wave basis and GGA[29] for the exchange–correlation energy. The cutoff energy of the plane waves was taken to be 19.11 Ry. Test calculations on bulk tin in the diamond structure gave the lattice constant and cohesive energy to be 6.63 Å and 3.157 eV/atom which are in excellent agreement with the experimental values[30] of 6.49 Å and 3.14 eV/atom, respectively. For clusters, we used a simple cubic supercell of side 20 Å and Γ point for the Brillouin zone integrations. A large number of structures, including those reported for Si[12] and Ge[10] clusters, were optimized.[14] It has been observed that hybrid exchange–correlation functional[31] like B3PW91 shows better agreement with that of experiments.[32] Therefore, the lowest energy structures obtained from GGA were reoptimized with B3PW91 exchange–correlation functionals using the Gaussian method.[33]

The calculated ground state structures of cation clusters were not significantly different from those of neutrals, though they were slightly deformed due to the odd number of electrons in these species.[32]

IV. RESULTS AND DISCUSSION

A. Incident energy dependence of SID profiles

SID profiles were investigated for Sn_x^+ ($x=4-20$) with incident energies ranging from nominal zero to 300 eV. In Fig. 1, incident energy dependence of SID patterns is exemplified by that of Sn_{13}^+. In the present experimental conditions, scattered parent ions were not resolved from those reflected by the electric field in the deceleration electrodes. At low incident energies, Sn_6^+ and Sn_7^+ were predominantly observed. This pattern is consistent with that observed by the photofragmentation experiment.[34] Hence, it is considered that these ions were generated by the unimolecular dissociation of the parent ion. With increasing E_i, the fragment mass spectra shifted to smaller mass regions, without exhibiting intense ions larger than Sn_7^+, which is indicative of successive fragmentations from Sn_6^+ and Sn_7^+. Further increase in E_i gave rise to intense mass peaks corresponding to Sn^+ and Sn_4^+. The spectral patterns did not change significantly for incident energies $E_i \geqslant 8$ eV/atom.

B. Low-energy SID profiles

Figure 2 shows the SID patterns for Sn_x^+ ($x=4-13$) with $E_i=0$ eV.[35] The fragmentation patterns in the Sn_{12}^+ and Sn_{13}^+ collisions are quite similar to those in SID for Si_{12}^+ and Si_{13}^+ collisions, which suggests an identical mechanism for

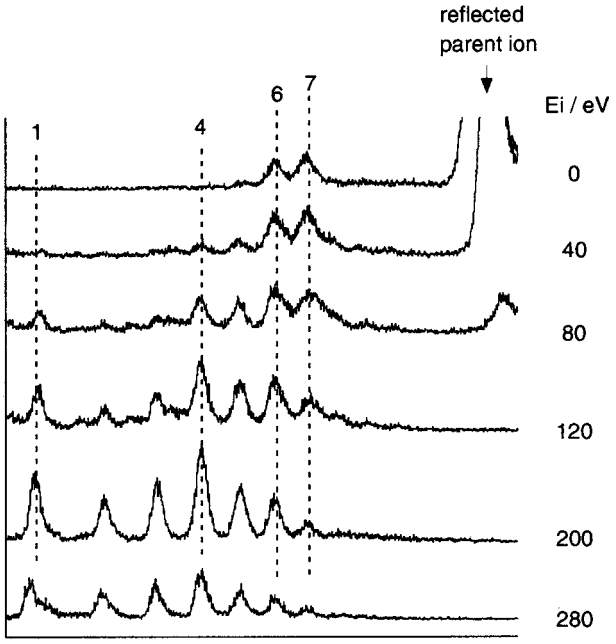

FIG. 1. Incident energy dependence of SID profiles for Sn_{13}^+.

fragmentation, the unimolecular decay, and similar structures and stability variations as a function of fragment size for both clusters.[15] The latter is rationalized by recent theoretical calculations performed for Si, Ge, and Sn clusters although several different ground state structures have been proposed.[7,12–14] As it can be seen in the figure, the fragmentation pattern drastically changes between Sn_{11}^+ and Sn_{12}^+:

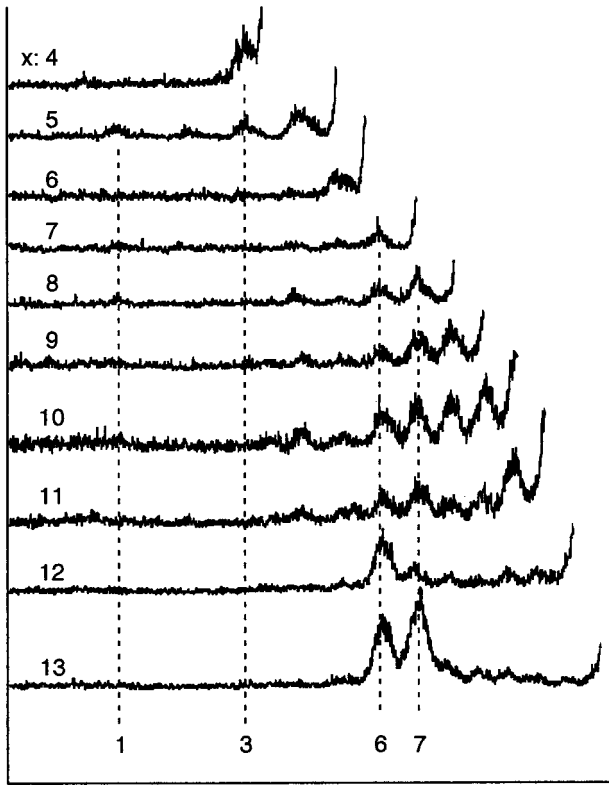

FIG. 2. SID profiles for Sn_x^+ ($x=4-13$) at the lowest incident energy (nominal 0 eV/atom).

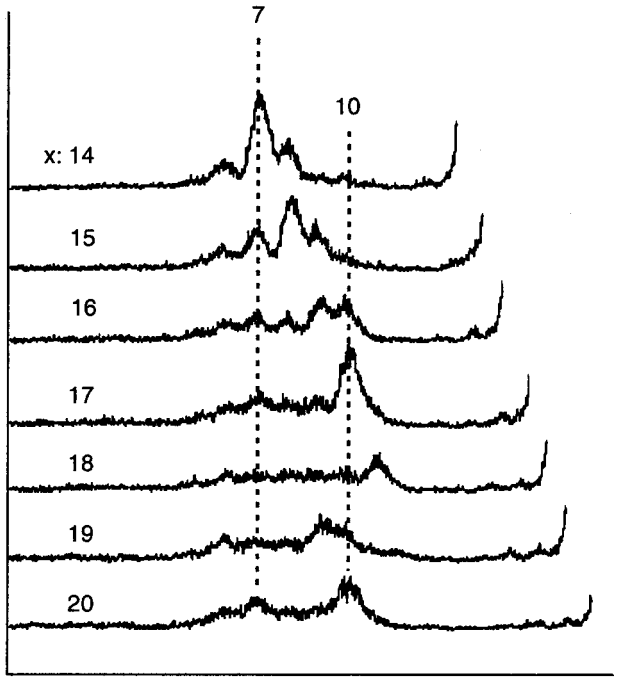

FIG. 3. SID profiles for Sn_x^+ ($x=14-20$) at the lowest incident energy (nominal 0 eV/atom).

Sn_6^+ and Sn_7^+ fragments were dominant for the Sn_{12}^+ and Sn_{13}^+ incidences, while fragments such as Sn_{x-1}^+, Sn_{x-2}^+, ... were the major species for the Sn_x^+ ($x=4-11$) incidences. The transition from the fission type to the atom loss type decay has been observed[36,37] in the CID patterns for Si_x^+ and Ge_x^+: the hexamer and heptamer fragment ions were dominant for $x \geqslant 9$ and 10 for Si_x^+ and Ge_x^+ respectively, and for x less than these values, mass peaks due to the atom loss process were comparable to or more intense than those of the hexamer and heptamer fragments. The atom loss process has often been observed in the unimolecular decay of metal clusters.[38–40] Thus, the result that the atom loss process was observed for a wider range of x for Sn_x^+ than Si_x^+ and Ge_x^+ may suggest that Sn_x^+ is more like clusters of metal elements than Si_x^+ and Ge_x^+ are.

In Fig. 3, low-energy SID patterns for Sn_x^+ ($x=14-20$) are shown. Fragment ions with $x=7-11$ were predominantly observed. This means that the parent clusters tend to decay into halves. In this size regime, the proposed ground state structures of Sn clusters consist of fused or stacked two subunits with almost identical sizes.[14] Thus, it seems reasonable that favored fragmentations may give rise to these stable subunit clusters. Among the fragmentation paths, those producing Sn_7, Sn_{10}, Sn_7^+, and Sn_{10}^+ were dominant. Similar results were reported for the low-energy CID of Si_x^+ and Ge_x^+, clusters.[36,37] Moreover, the most intense fragment peaks observed for the parent ions were almost the same as those for the corresponding Si and Ge cluster ions.[36,37] All Si, Ge, and Sn pentamer and decamer are at local minima in the second order difference of the total energy $[\Delta E_2 = 2E(x) - E(x+1) - E(x-1)]$.[7,13,14] It is also predicted by the present calculation that ΔE_2 is minimal at Sn_7^+, and Sn_{10}^+.[32]

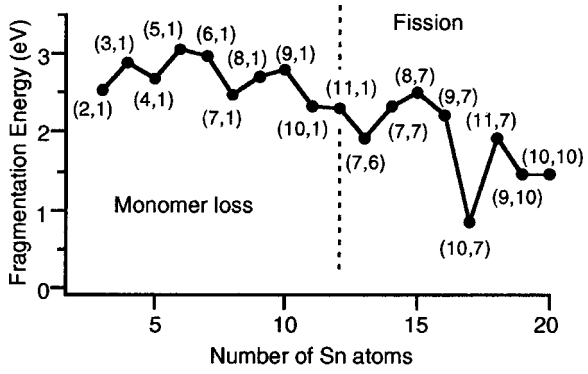

FIG. 4. Fragmentation energies for the lowest fragmentation channels derived from the calculations using B3PW91 hybrid energy functionals.

C. Comparison with the calculated fragmentation paths

Figure 4 shows the most favored fragmentation channels for tin cluster cations into a cation and a neutral product. Table I gives a comparison of the observed fragmentation paths with a few lowest energy fragmentation channels obtained from the B3PW91 calculations. Assuming that fragmentation occurs along the lowest energy pathways with no activation barrier, we calculated the fragmentation energy, $E_f(x^+)=E(x^+)\text{-}E(y^+)\text{-}E(z)$, of an x-atom cation cluster into a y-cation and a z-neutral cluster product $(x=y+z)$. Comparison with the experimental results shows that B3PW91 results are in better agreement as compared to the earlier results where only neutral clusters were considered.[14] It is found that in both cases Sn_x^+ clusters with $x\leqslant 11$ favor monomer evaporation, while for larger clusters, a fission-type fragmentation is more favorable. For Sn_{12}^+, the monomer loss process was more favored in calculation than the fission to Sn_6^+ and Sn_6. However, the fragmentation energy difference between the two processes was as small as 0.2–0.3 eV. This is consistent with the experimental result that Sn_{12}^+ are at the border of the two types of decay. Among all the fragmentation channels in Fig. 4, abnormally low fragmentation energy for Sn_{17}^+ is conspicuous. This is due to high stabilities of both Sn_{10}^+ and Sn_7 fragments.

It should be noted that the present calculation using B3PW91 functionals predicts that the charge should be on the heavier fragment in the monomer loss processes. However, in GGA, charge was predicted to be on monomers, and it is only for the heavier parent ions that GGA results were in agreement with experiment. This is due to a better prediction of the IPs using B3PW91 functional.[32]

For the present estimate of the fragmentation energy, only cohesive energies of the lowest-energy geometries are considered, assuming that there are no activation barriers. Though the estimate gives a significant insight into the lowest-energy SID processes, it fails to predict the higher energy spectra, as is apparent in Fig. 1. Unimolecular decays from the fission fragments, Sn_6^+ and Sn_7^+, seem to occur at $E_i>40$ eV. However, such successive decays need significantly larger energies than single fissions giving such as $Sn_9^+ + Sn_4$, which is not apparent throughout the incident energies studied. This is in contrast to SID of small carbon cluster anions in which the fragmentation patterns are explained by single fissions up to a medium collision energy range (6–10 eV/atom).[17] Details of the fragmentation dynamics must be considered for understanding the SID patterns at high incident energies.

TABLE I. Comparison of favored fragmentation channels obtained from the calculation and the experiment.

x	Calculation	Experiment
3	(2,1)	
4	(3,1)	(3,1)
5	(4,1)	(4,1)(3,2)
6	(5,1)	(5,1)
7	(6,1)	(6,1)
8	(7,1)	(7,1)
9	(8,1)	(8,1)(7,2)
10	(9,1)	(9,1),(8,2),(7,3)
11	(10,1)	(10,1),(7,4),(6,5)
12	(11,1),(7,5),(6,6)	(6,6)
13	(7,6)(6,7)	(7,6)(6,7)
14	(7,7)	(7,7)
15	(8,7)(9,6)	(8,7),(9,6),(7,8)
16	(9,7),(10,6)	(9,7),(10,6)
17	(10,7)	(10,7)
18	(11,7)(8,10)	(11,7)
29	(10,9)	(9,10),(10,9)
20	(10,10)	(10,10)

D. High-energy SID profiles

At high incident energies ($\geqslant 8$ eV/atom), small fragment ions, mainly with $x=1-4$, were observed for all the parent ions with $x=8-20$. The relative intensities of the mass peaks did not depend significantly on the sizes of the parent clusters and the incident energies. Figure 5 summarizes the mass spectra for the scattered cluster ions at $E_i\approx 12$ eV/atom. The intensities of the Sn_4^+ fragment ions were higher than those of the adjacent ions. The enhancement of the Sn_4^+ ion peak was reported for the mass abundance patterns of Sn cluster ions from the liquid metal ion.[41] The relative abundances of $Sn^+-Sn_4^+$ fragment ions in Fig. 5 were similar to those in a mass spectrum obtained by the high fluence laser ionization of neutral clusters.[2] At this high energy, successive fragmentations of the parent ions are expected to occur. Thus, the relative intensities of the fragment mass peaks are expected to correlate with the resistivity of the clusters to fragmentation. As shown in Fig. 4, our calculations predict a larger fragmentation energy for Sn_4^+ than for Sn_3^+ and Sn_5^+. This supports the enhancement of the Sn_4^+ ion peak in the successive unimolecular decay.

The incident energy dependence of SID patterns for Sn_{13}^+ is weak for incident energies higher than 120 eV as shown in Fig. 1. This behavior implies that the internal energy of the scattered clusters is not changed significantly by changing incident energy (E_i). This can be understood by considering an ion implantation threshold reported for the collision of Ag_x^+ clusters with an HOPG surface.[20,42,43] For this system, the deposition yields of clusters as a function of ion collision energy have been studied in detail, and it has been shown

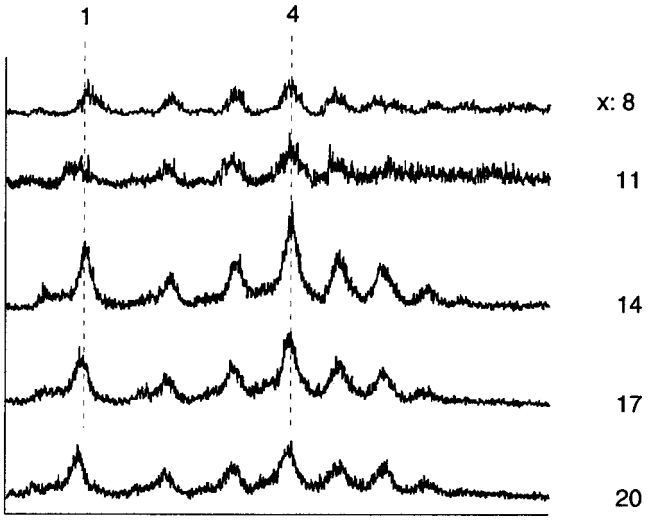

FIG. 5. SID profiles for Sn_x^+ (x=8, 11, 14, 17, and 20) at a high incident energy ($\approx$12 eV/atom).

that, with increasing collision energy, the scattering yield of clusters abruptly decreases at a certain collision energy; above this energy, cluster ions are considered to be implanted in the HOPG substrate (implantation threshold). Although the details of the cluster-surface interactions are not known for the present system, similar implantation behavior for Sn_x^+ can be expected with the same substrate, HOPG. Since projectile ions with energies higher than the threshold energies are implanted into the substrate, the increment in averaged collision energy for the scattered ions can be much smaller than that in E_i. This can result in the weak incident energy dependence of the mass patterns for $E_i > 120$ eV.

V. CONCLUSION

Fragmentation profiles in low-energy (0–300 eV) collisions of Sn_x^+ ($x=4-20$) with a highly oriented pyrolytic graphite (HOPG) surface have been investigated. The favored fragmentation paths were similar to those for Si and Ge cluster ions in the CID studies.[36,37] The result supports the structural similarities among Si, Ge, and Sn clusters in the present size range, although the proposed structures are not perfectly identical.[12–14]

The low-energy SID patterns were in excellent agreement with the fragmentation energy calculated using B3PW91 hybrid functionals, while GGA failed to reproduce the experimental results in the smaller size range. This is probably because electron correlation is more important for smaller size range and metallic nature of bonding emerges for clusters with larger sizes.[32]

ACKNOWLEDGMENTS

Two of the authors (C.M. and V.K.) acknowledge the kind hospitality at the Institute for Materials Research and the Staff of the Center for Computational Materials Science at IMR–Tohoku University for making the Hitachi SR2201 and SR8000 parallel machines available and for their cooperation.

[1] See, for example, F. A. Cotton, G. Wilkinson, C. A. Murillo, and M. Bochmann, *Advanced Inorganic Chemistry*, 6th ed. (Wiley, New York, 1999), p. 207.
[2] K. LaiHing, R. G. Wheeler, W. L. Wilson, and M. A. Duncan, J. Chem. Phys. **87**, 3401 (1987).
[3] M. Sakurai, K. Watanabe, K. Sumiyama, and K. Suzuki, J. Chem. Phys. **111**, 235 (1999).
[4] B. Wang, L. M. Molina, M. J. Lopez, A. Rubio. J. A. Alonso, and M. J. Scott, Ann. Phys. (Leipzig) **7**, 107 (1998).
[5] G. Ganteför, M. Gausa, K. H. Meiwes-Broer, and H. O. Lutz, Z. Phys. D: At., Mol. Clusters **12**, 405 (1989).
[6] Ch. Lüder and K. H. Meiwes-Broer, Chem. Phys. Lett. **294**, 391 (1998).
[7] Z.-Y. Lu, C.-Z. Wang, and K.-M. Ho, Phys. Rev. B **61**, 2329 (2000).
[8] G. von Helden, M.-T. Hsu, P. R. Kemper, and M. T. Bowers, J. Chem. Phys. **95**, 3835 (1991).
[9] Ph. Dugourd, R. R. Hudgins, J. M. Tenenbaum, and M. F. Jarrold, Phys. Rev. Lett. **80**, 4197 (1998).
[10] A. A. Shvartsburg, B. Liu, Z.-Y. Lu, C.-Z. Wang, M. F. Jarrold, and K.-M. Ho, Phys. Rev. Lett. **83**, 2167 (1999).
[11] A. A. Shvartsburg and M. F. Jarrold, Chem. Phys. Lett. **317**, 615 (2000).
[12] B. Liu, Z.-Y. Lu, B. Pan, C.-Z. Wang, K.-M. Ho, A. A. Shvartsburg, and M. F. Jarrold, J. Chem. Phys. **109**, 9401 (1998); K.-M. Ho, A. A. Shvartsburg, B. Pan, Z.-Y. Lu, C.-Z. Wang, J. G. Wacker, J. L. Fye, and M. F. Jarrold, Nature (London) **392**, 582 (1998).
[13] J. Wang, G. Wang, and J. Zhao, Phys. Rev. B **64**, 205411 (2001).
[14] C. Majumder, V. Kumar, H. Mizuseki, and Y. Kawazoe, Phys. Rev. B **64**, 233405 (2001).
[15] P. M. St. John and R. L. Whetten, Chem. Phys. Lett. **196**, 330 (1992).
[16] T. M. Bernhardt, B. Kaiser, and K. Rademann, Z. Phys. Chem. (Munich) **195**, 273 (1996).
[17] Y. Tai, J. Murakami, Y. Maruyama, W. Yamaguchi, T. Mizota, K. Igarashi, and S. Tanemura, J. Phys. Chem. B **103**, 5500 (1999).
[18] Y. Tai and J. Murakami, Chem. Phys. Lett. **339**, 9 (2001).
[19] A. A. Shvartsburg, M. F. Jarrold, B. Liu, Z.-Y. Lu, C.-Z. Wang, and K.-M. Ho, Phys. Rev. Lett. **81**, 4616 (1998).
[20] Y. Tai, W. Yamaguchi, Y. Maruyama, K. Yoshimura, and J. Murakami, J. Chem. Phys. **113**, 3808 (2000).
[21] J. B. Hopkins, P. R. R. Langridge-Smith, M. D. Morse, R. E. Smalley, J. Chem. Phys. **78**, 1627 (1983).
[22] W. C. Wiley and I. H. McLaren, Rev. Sci. Instrum. **26**, 1150 (1955).
[23] B. Kaiser, T. M. Bernhardt, and K. Rademann, Nucl. Instrum. Methods Phys. Res. B **125**, 223 (1997).
[24] H. Danigel, H. Jungclas, and L. Schmidt, Int. J. Mass Spectrom. Ion Phys. **52**, 223 (1983).
[25] S. R. Keleman, H. Freund, and C. A. Mims, J. Vac. Sci. Technol. A **2**, 987 (1984).
[26] D. V. Chakarov, L. Oesterlund, and B. Kasemo, Vacuum **46**, 1109 (1995).
[27] Vienna *ab initio* simulation package, Technische Universitä at Wien, 1999; G. Kresse and J. Furthmüller, Phys. Rev. B **54**, 11 169 (1996).
[28] D. Vanderbilt, Phys. Rev. B **41**, 7892 (1990).
[29] J. P. Perdew, in *Electronic Structure of Solids '91,* edited by P. Ziesche and H. Eschrig (Akademie Verlag, Berlin, 1991).
[30] C. Kittel, *Introduction to Solid State Physics,* 7th ed. (Wiley, New York, 1996), p. 57.
[31] A. D. Becke, Phys. Rev. A **38**, 3098 (1988); C. Lee, W. Yang and R. G. Parr, Phys. Rev. B **37**, 785 (1988); A. D. Becke, J. Chem. Phys. **98**, 5648 (1993); K. Burke, J. P. Perdew, and Y. Wang, in *Electronic Density Functional Theory: Recent Progress and New Directions*, edited by J. F. Dobson, G. Vignale, and M. P. Das (Plenum, New York, 1998); J. P. Perdew, J. A. Chevary, S. H. Vosko, K. A. Jackson, M. R. Pederson, D. J. Singh and C. Fiolhais, Phys. Rev. B **46**, 6671 (1992); J. P. Perdew, in *Electronic Structure of Solids '91*, edited by P. Ziesche and H. Eschrig (Akademie Verlag, Berlin, 1991), p. 11; J. P. Perdew, J. A. Chevary, S. H. Vosko, K. A. Jackson, M. R. Pederson, D. J. Singh and C. Fiolhais, Phys. Rev. B **48**, 4978 (1993); J. P. Perdew, K. Burke and Y. Wang, Phys. Rev. B **54**, 16533 (1996).
[32] C. Majumder, V. Kumar, H. Mizuseki, and Y. Kawazoe (unpublished).
[33] M. J. Frisch, G. W. Trucks, H. B. Schlegel *et al.*, GAUSSIAN 98, Revision A.10, Gaussian, Inc., Pittsburgh, PA, 2001.
[34] S. Yoshida and K. Fuke, Trans. Mater. Res. Soc. Jpn. **25**, 995 (2000).
[35] At this collision energy, only the half of the incident ions with higher

kinetic energies collide with the surface. The collision energy of such ions averaged over the distribution is ≈29 eV.
[36] M. F. Jarrold and J. E. Bower, J. Phys. Chem. **92**, 5702 (1988).
[37] J. M. Hunter, J. L. Fye, M. F. Jarrold, and J. E. Bower, Phys. Rev. Lett. **73**, 2063 (1994).
[38] P. J. Brucat, L.-S. Zheng, C. L. Pettiette, S. Yang, and R. E. Smalley, J. Chem. Phys. **84**, 3078 (1985).
[39] S. K. Loh and P. B. Armentrout, J. Am. Chem. Soc. **111**, 3167 (1989).
[40] O. Ingolfsson, U. Busolt, and K. Sugawara, J. Chem. Phys. **112**, 4613 (2000).
[41] M. Watanabe, Y. Saito, S. Nishigaki, and T. Noda, Jpn. J. Appl. Phys. Part 1 **27**, 344 (1988).
[42] W. Yamaguchi, K. Yoshimura, Y. Tai, Y. Maruyama, K. Igarashi, S. Tanemura, and J. Murakami, J. Chem. Phys. **112**, 9961 (2000).
[43] S. J. Carroll, S. Pratontep, M. Streun, and R. E. Palmer, J. Chem. Phys. **113**, 7723 (2000).